CMS Physics Analysis Summary

Contact: cms-pag-conveners-higgs@cern.ch 2011/03/11

Search For Neutral MSSM Higgs Boson Production via Decays to Tau Pairs in pp Collisions at $\sqrt{s} = 7$ TeV

The CMS Collaboration

Abstract

The results of a search for neutral MSSM Higgs boson production in pp collisions at the LHC at a center-of-mass energy of 7 TeV are presented, based on a data sample corresponding to an integrated luminosity of 36 pb^{-1}. We search for decays of the Higgs bosons to tau lepton pairs, using the final states with one identified e or μ from leptonic tau decay plus a reconstructed hadronic decay of a tau lepton, and also the final state with two leptonic tau decays, and then fully reconstruct the original tau lepton pair kinematics using a novel likelihood algorithm. No excess is observed in the fully reconstructed tau pair invariant mass spectrum. The resulting upper bounds on the Higgs production cross section times branching ratio to tau pairs as a function of the Higgs boson mass yield stringent new bounds in the MSSM parameter space m_A versus $\tan\beta$, extending as low as $\tan\beta = 23$ for $m_A = 130\ \text{GeV}/c^2$.

1 Introduction

The standard model (SM) has been extremely successful in describing a wide range of phenomena in particle physics, and has survived some three decades of experimental testing. But the main remaining undiscovered particle predicted by the SM, the Higgs boson [1–5], suffers from quadratically divergent self-energy corrections at high energies [6]. Numerous extensions to the SM have been proposed to address these divergences. One such model, supersymmetry [7], a symmetry between fundamental bosons and fermions, results in cancellation of the divergences at tree level. The minimal supersymmetric extension to the standard model (MSSM) requires the presence of two Higgs doublets. This leads to a more complicated Higgs boson sector, with five massive Higgs bosons: a light neutral scalar (h), two charged scalars ($H^{\pm}$), a heavy neutral CP-even state (H) and a neutral CP-odd state (A).

The masses of the MSSM Higgs boson states are specified up to radiative corrections mainly by two parameters, usually taken to be the mass of the pseudoscalar state, m_A, and the ratio of the vacuum expectation values of the two Higgs doublets, $\tan\beta$. At large $\tan\beta$ (greater than about 20–30) the couplings of the Higgs bosons to down-type quarks are proportional to $\tan\beta$. As a result the cross section for two of the three neutral Higgs bosons can be nearly as large as that for electroweak gauge bosons (W, Z) production at a proton-proton collider such as the Large Hadron Collider (LHC). Two main production processes contribute to $pp \to \phi + X$, where $\phi = h, H$, or A: gg fusion through a b-quark loop and direct $b\bar{b}$ annihilation from the b parton density in the incoming beam protons.

The mass relations among the neutral MSSM Higgs bosons are such that if $m_A \lesssim 130\,\mathrm{GeV}/c^2$, at large $\tan\beta$ the masses of the h and A are nearly degenerate, while that of the H is approximately 130 GeV/c^2. If $m_A \gtrsim 130$ GeV/c^2 then the masses of the A and H are nearly degenerate while that of the h remains near 130 GeV/c^2. The precise value of the crossover point depends predominantly on the nature of the mass mixing in the top squark states.

This note reports a search for MSSM neutral Higgs bosons in pp collisions at $\sqrt{s} = 7$ TeV at the LHC in 2010, using a data sample corresponding to 36 pb^{-1} of integrated luminosity recorded by the Compact Muon Solenoid (CMS) experiment. This search is similar to those performed at the Tevatron [8] and complementary to the MSSM Higgs search at LEP2 [9].

The tau pair decays of the neutral Higgs bosons, having a branching ratio of about 10%, serve as the best experimental signature for this search. The $b\bar{b}$ mode, though it has a much larger branching ratio, suffers from overwhelming background from QCD processes. Three final states where the τ decays leptonically or hadronically are used: $e\tau_h$, $\mu\tau_h$, and $e\mu$, where we use the symbol τ_h to indicate a reconstructed hadronic decay of a tau. The ee and $\mu\mu$ final states suffer too much background from $Z/\gamma^* \to \ell\ell$ events to be usable.

The CMS detector has an overall cylindrical geometry surrounding the pp collision region, with charged particle tracking detectors, electromagnetic calorimetry and hadron calorimetry all lying inside a 3.8 T magnetic field from a superconducting solenoid. Outside the solenoid, embedded in the steel magnetic field return yoke, are layers of muon detectors. Details of the CMS detector and its performance can be found elsewhere [10].

We use a coordinate system in which the counterclockwise proton beam (viewed from above) is along the z axis, and we measure the pseudorapidity η of outgoing particles based on their polar angle θ to the z axis according to $\eta \equiv -\ln\tan\frac{\theta}{2}$. The transverse plane is denoted by the subscript T on kinematic quantities.

2 Triggers and Event Selection

The triggers used to select the events for this analysis are based on the presence of a muon and/or an electron trigger object [11, 12]. With increasing instantaneous luminosity, in order to keep the online thresholds on electrons lower than those used in offline selections, special triggers requiring the presence of both a lepton and a charged track and calorimeter pattern consistent with a tau decaying hadronically were adopted.

The analysis presented here makes use of particle flow techniques which combine the information from all CMS subdetectors to identify and reconstruct individual particles in the event, namely muons, electrons, photons, and charged and neutral hadrons. The detailed description of the algorithm and its commissioning can be found elsewhere [13, 14]. The particle list is then given as input to the jet, tau, and transverse missing energy reconstruction.

The main challenge in the identification of hadronic tau decays is overcoming the large background from hadronic jets from QCD processes. Hadronic tau decays yield one or three charged pions, plus zero to several neutral pions, depending on the decay mode. The algorithm used here, called HPS [15], is described in Appendix 1.

For the $\mu\tau_h$ and $e\tau_h$ final states, we select events with an isolated muon or electron with $p_T > 15$ GeV/c and $|\eta| < 2.1$, and an oppositely-charged τ_h with $p_T > 20$ GeV/c and $|\eta| < 2.3$. The transverse mass of the $\ell = e, \mu$ with the missing transverse energy E_T^{miss} is defined as $M_T = \sqrt{2p_T^{\ell} E_T^{miss} \cdot (1 - \cos\Delta\phi)}$, where $\Delta\phi$ is the difference in azimuth between the e or μ and the E_T^{miss} vector. We require $M_T < 40$ GeV/c^2, in order to reduce the background from W+jets events. For the $e\mu$ final state, we select events with an isolated electron with $|\eta| < 2.5$ and an oppositely charged isolated muon, both with $p_T > 15$ GeV/c, and $M_T < 50$ GeV/c^2, calculated for each lepton separately. We reject events in which there are more than one e or μ.

3 Backgrounds

The observed number of events in each channel appears in Table 1. The largest single source of events selected with these requirements come from $Z \to \tau\tau$. We estimate the contribution from this process using a detailed GEANT4 simulation of the CMS detector, with the events modeled using the POWHEG Monte Carlo generator. We use a normalization for this process based on the number of observed $Z \to \mu\mu$ events [16].

A significant background arises from hadronic multijet events from QCD processes in which the jets are misidentified as τ_h and there is a high-p_T real or misidentified e or μ, and W+jets events in which the jet is misidentified as a τ_h. The rates for these processes are estimated using the ratio of same-charge to opposite-charge events, and cross-checked using the jet-to-tau misidentification rate measured in multijet events. Other background processes include $t\bar{t}$ production and $Z \to ee/\mu\mu$ events. Table 1 shows the expected number of events for all background processes. The event generator PYTHIA6 [17] is used to model Higgs signal and other backgrounds. The TAUOLA [18] package is used for tau decays in all cases.

4 Invariant Mass Reconstruction and Fit

To distinguish the Higgs boson signal from the background we reconstruct the tau pair mass using a likelihood technique, described in Appendix 2. The algorithm determines the original tau three-momenta by maximizing a likelihood with respect to free parameters corresponding

Table 1: The number of estimated background events in the selected sample for each channel, the observed number of events, and the overall signal efficiency for $m_A = 120\,\mathrm{GeV}/c^2$ (including branching ratios). Uncertainties do not include those on integrated luminosity or energy scales. The multijet background for the $e\tau_h$ final state is the sum of the QCD multijet and γ+jet backgrounds.

Process	$\mu\tau_h$	$e\tau_h$	$e\mu$
$Z \to \tau\tau$	329 ± 77	190 ± 44	88 ± 5
$t\bar{t}$	6 ± 3	2.6 ± 1.3	7.1 ± 1.3
$Z \to \ell\ell$, $jet \to \tau_h$	6.4 ± 2.4	15 ± 6.2	
$Z \to \ell\ell$, $\ell \to \tau_h$	13.3 ± 3.6	119 ± 28	
$W \to \ell\nu$	54.9 ± 4.8	30.6 ± 3.1	
$W \to \tau_\ell\nu$	14.7 ± 1.3	7.0 ± 0.7	3.9 ± 1.2
QCD	132 ± 14	181 ± 23	
$WW/WZ/ZZ$	1.6 ± 0.8	0.8 ± 0.4	3.0 ± 0.4
Total	558 ± 79	546 ± 57	102 ± 5
Observed	540	517	101
Signal Efficiency ($m_A = 120\,\mathrm{GeV}/c^2$)	0.0253	0.0156	0.00561

to the missing tau neutrino momenta, and subject to all applicable kinematic constraints. Other terms in the likelihood take into account the tau decay phase space and probability density in tau transverse momentum, parametrized as a function of tau pair mass. This algorithm results in a tau pair mass with a mean consistent with the true tau pair mass, and a nearly Gaussian shape. The observed reconstructed tau pair mass distribution for all three channels is shown in Fig. 1.

5 Systematic Uncertainties

Various imperfectly known or imperfectly simulated effects can alter the shape and normalization of the reconstructed tau pair mass spectrum. The main sources of normalization uncertainties include the total integrated luminosity (11%), background normalizations (Table 1), Z production cross section (4%) and lepton identification and isolation efficiency (0.2–2.0% depending on lepton type). We estimate the tau identification efficiency uncertainty to be 23% from an independent measurement [19]. Uncertainties that contribute to shape variations include tau (3%) and lepton energy scale (1–2% depending on lepton type), and uncertainties on the E_T^{miss} scale that is used for the tau pair invariant mass reconstruction [20]. The E_T^{miss} scale uncertainties contribute via the jet energy scale (3%) and unclustered energy scale (10%) where unclustered energy is defined as the energy remaining after vectorially subtracting leptons and objects clustered in jets with $p_T > 10\,\mathrm{GeV}/c$.

To search for the presence of a Higgs boson signal in the selected events we perform likelihood fit to the tau pair invariant mass spectrum. Systematic uncertainties are represented by nuisance parameters, which we remove by marginalization, assuming a log normal prior for normalization parameters, and Gaussian priors for mass spectrum shape uncertainties. The uncertainties that affect the shape of the mass spectrum, mainly those corresponding to the energy scales, are represented by nuisance parameters which result in a continuous modification of the spectrum shape [21].

The parameter representing the tau identification uncertainty affects taus from the Higgs boson

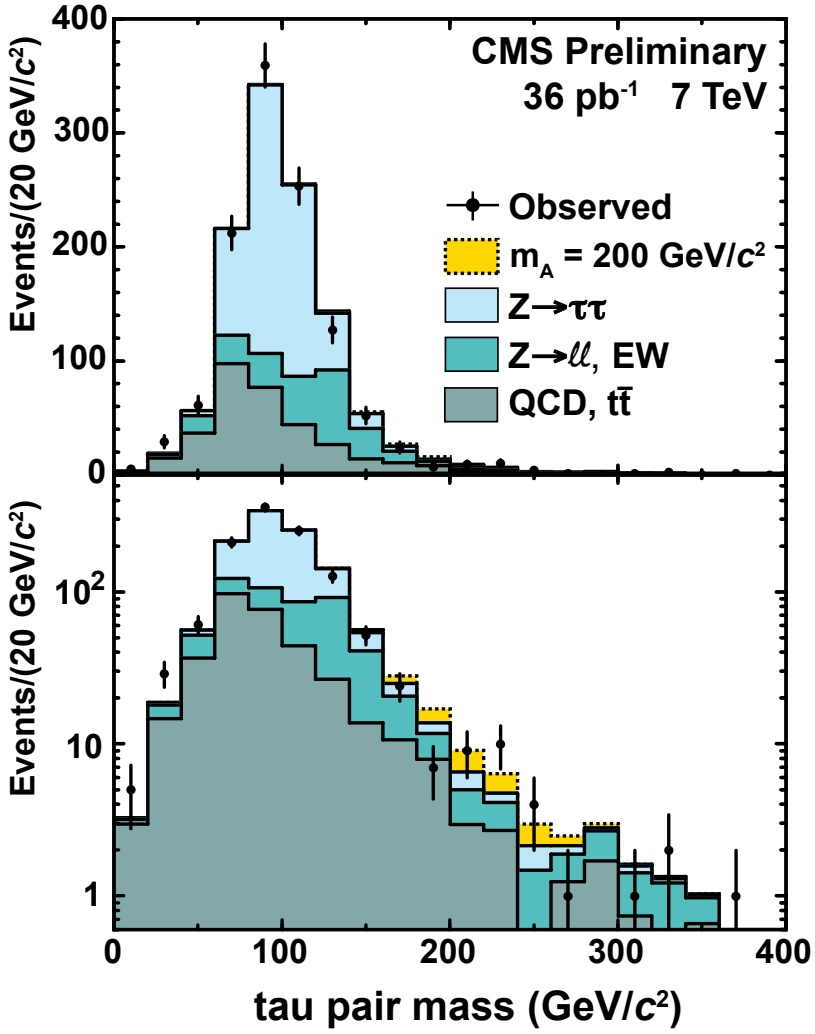

Figure 1: The reconstructed tau pair invariant mass distribution on linear (above) and log (below) scales, for the sum of the $e\tau_h$, $\mu\tau_h$, and $e\mu$ final states, comparing the observed distributions (data points with error bars) to the sum of the expected backgrounds (shaded histograms). The contribution from a Higgs boson signal ($m_A = 200$ GeV$/c^2$) is also shown, with normalization corresponding to the 95% upper bound.

signal and the main background, $Z \to \tau\tau$, equally. This effectively allows the observed $Z \to \tau\tau$ events to provide an *in situ* calibration of this efficiency, except for Higgs masses near that of the Z. Near the Z mass, the tau identification efficiency uncertainty dominates in the $e\tau_h$ and $\mu\tau_h$ channels and the $e\mu$ channel provides the greatest sensitivity.

6 Results

The mass spectra show no evidence for the presence of a Higgs boson signal, and we set 95% C.L. upper bounds on the Higgs boson cross section times the tau pair branching ratio (denoted $\sigma_\phi \cdot B_{\tau\tau}$) using a Bayesian method assuming a uniform prior in $\sigma_\phi \cdot B_{\tau\tau}$. The invariant mass spectrum in Fig. 1 shows the contribution of a Higgs boson signal corresponding to m_A = 200 GeV/c^2 with $\sigma_\phi \cdot B_{\tau\tau} = 8.71$ pb, the value above which we exclude at 95% C.L.

Figure 2 shows the observed 95% C.L. upper bound on $\sigma_\phi \cdot B_{\tau\tau}$ as a function of m_A, where we use as our signal acceptance model the combined spectra from the gg and $b\bar{b}$ production processes for h, A, and H, assuming $\tan\beta = 30$ [22]. The plot also shows the one- and two-standard deviation range of expected upper limits for various potential experimental outcomes. The observed limits are well within the expected range assuming no signal. The observed and expected upper limits are shown in Table 2.

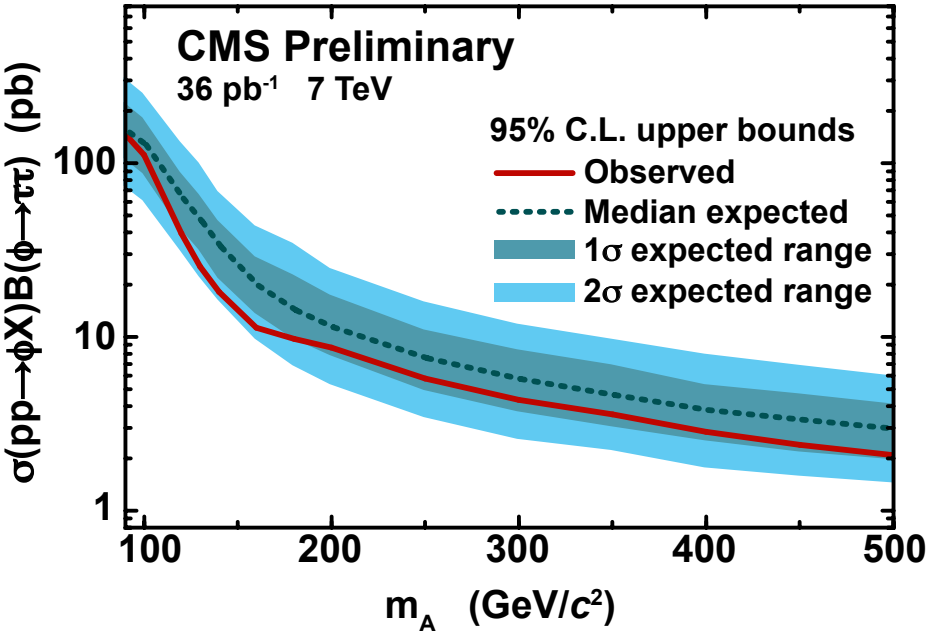

Figure 2: The expected one- and two-standard-deviation ranges (blue bands) and observed (red line) 95% C.L. upper limits on $\sigma_\phi \cdot B_{\tau\tau}$ as a function of m_A.

We can interpret the upper limits on $\sigma_\phi \cdot B_{\tau\tau}$ in the MSSM parameter space of $\tan\beta$ versus m_A for an example scenario. We use here the m_h^{max} [23] benchmark scenario in which M_{SUSY} = 1 TeV/c^2; X_{PQt} = 2M_{SUSY}; μ = 200 GeV/c^2; $M_{\tilde{g}}$ = 800 GeV/c^2; M_2 = 200 GeV/c^2; and $A_b = A_t$, where M_{SUSY} denotes the common soft-SUSY-breaking squark mass of the third generation; $X_t = A_t\mu/\tan\beta$ the stop mixing parameter; A_t and A_b the stop and sbottom trilinear couplings, respectively; μ the Higgsino mass parameter; $M_{\tilde{g}}$ the gluino mass; and M_2 the SU(2)-gaugino mass parameter. The value of M_1 is fixed via the GUT relation $M_1 = (5/3)M_2 \sin\theta_w/\cos\theta_w$.

95% C.L. Upper Limit (pb)							
m_A	Expected $\sigma_\phi \cdot B_{\tau\tau}$ (pb)					Observed	
(GeV/c^2)	-2σ	-1σ	median	+1σ	+2σ	$\sigma_\phi \cdot B_{\tau\tau}$ (pb)	$\tan\beta$
90	74.90	107.75	153.30	227.10	315.33	147.74	27.36
100	61.59	88.61	127.09	184.17	256.05	112.30	29.20
120	31.96	42.72	62.48	90.24	135.24	39.61	25.22
130	22.60	31.97	45.96	67.11	101.60	25.40	22.57
140	16.58	22.14	32.81	47.30	69.83	18.20	23.55
160	9.88	13.83	19.70	29.27	44.29	11.37	23.83
180	6.93	9.95	14.16	23.13	35.12	9.78	28.08
200	5.41	7.90	11.36	17.61	25.10	8.71	32.98
250	3.49	5.01	7.54	11.15	16.11	5.77	43.35
300	2.62	3.77	5.71	8.58	12.06	4.36	56.62
350	2.26	3.09	4.64	7.04	9.85	3.60	-
400	1.79	2.57	3.79	5.39	8.07	2.86	-
450	1.61	2.21	3.34	4.77	6.95	2.41	-
500	1.47	2.00	2.95	4.18	6.06	2.10	-

Table 2: Expected one- and two-standard-deviation range, and observed 95% C.L. upper limits on $\sigma_\phi \cdot B_{\tau\tau}$ as functions of m_A, and 95% C.L. upper bound on MSSM parameter $\tan\beta$ in the m_h^{max} scenario described in the text. No bounds on $\tan\beta$ above 60 are quoted.

In determining these bounds on $\tan\beta$, which are shown in Table 2 and in Fig. 3, we have used the central values of the cross sections as a function of $\tan\beta$ reported by the LHC Higgs Cross Section Working Group [22, 24–30]. The effect of the theoretical uncertainties is illustrated in Fig. 3.

The excluded region in $\tan\beta$ extends down to values smaller than those excluded by the Tevatron experiments [8] for $m_A \lesssim 140$ GeVc^2, and the present results significantly extend the excluded region of MSSM parameter space at larger values of m_A. The plot also shows the region excluded by the LEP2 experiments [9].

7 Conclusion

We have used the first sample of CMS physics data from proton-proton collisions at 7 TeV center-of-mass energy at the LHC, corresponding to an integrated luminosity of 36 pb^{-1}, to search for neutral Higgs production using the tau pair decay mode in final states with one e or μ plus a hadronic decay of a tau, and the $e\mu$ final state. The observed tau pair mass spectrum reveals no evidence for neutral Higgs boson production, and we determine 95% C.L. upper bounds on the product of the Higgs boson cross section and tau pair branching ratio as a function of m_A. These results, interpreted in the MSSM parameter space of $\tan\beta$ versus m_A, exclude a previously unexplored region reaching as low as $\tan\beta = 23$ at $m_A = 130$ GeV/c^2.

References

[1] P. W. Higgs *Phys. Rev. Lett.* **12** (1964) 132.

[2] P. W. Higgs *Phys. Rev. Lett.* **13** (1964) 508.

[3] F. Englert and R. Brout *Phys. Rev. Lett.* **13** (1964) 321.

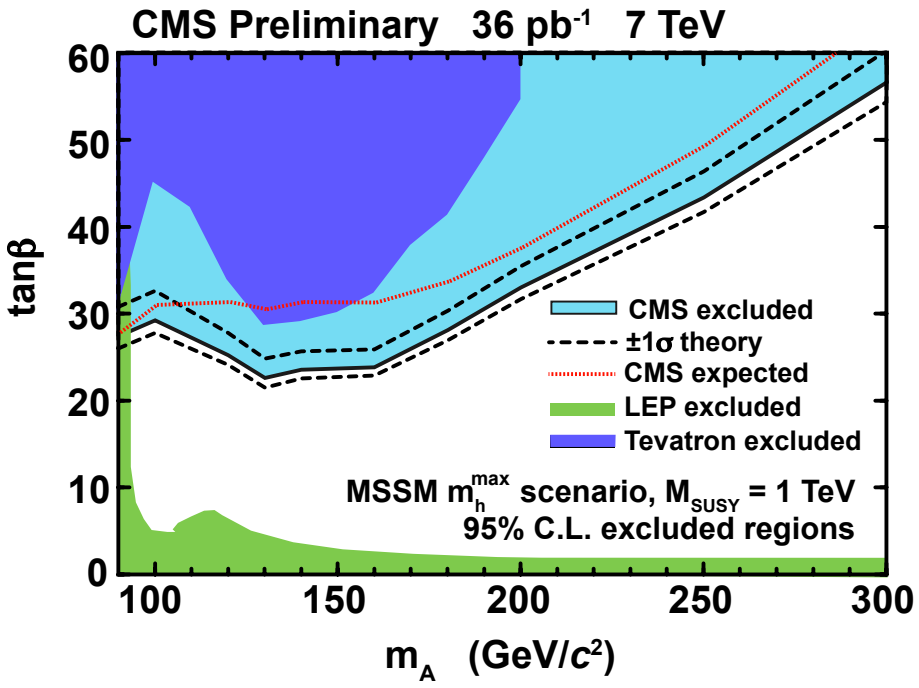

Figure 3: Region in the parameter space of tan β versus m_A excluded at 95% C.L. in the context of the MSSM m_h^{max} scenario, with the effect of $\pm 1\sigma$ theoretical uncertainties shown. The other shaded regions show the 95% C.L. excluded regions from the LEP and Tevatron experiments.

[4] G. Guralnik, C. Hagen, and T. Kibble *Phys. Rev. Lett.* **13** (1964) 585.

[5] P. W. Higgs *Phys. Rev.* **145** (1966) 1156.

[6] E. Witten *Phys. Lett. B* **105** (1981) 267.

[7] S. P. Martin, "A Supersymmetry Primer", *arXiv:hep-ph/9709356* (1997). and references therein.

[8] CDF and D0 Collaboration *arXiv:hep-ex/1003.3363* (2010).

[9] LEP Higgs Working Group Collaboration *Eur. Phys. J.* **C47** (2006) 547–587.

[10] CMS Collaboration, "The CMS experiment at the CERN LHC", *J. Instrum.* **0803:S08004** (2008).

[11] CMS Collaboration, "Electron reconstruction and identification at sqrt(s) = 7 TeV", *CMS Physics Analysis Summary* **EGM-10-004** (2010).

[12] CMS Collaboration, "Performance of muon identification in pp collisions at $\sqrt{s} = 7$ TeV", *CMS Physics Analysis Summary* **MUO-10-002** (2010).

[13] CMS Collaboration, "Particle-Flow Event Reconstruction in CMS and Performance for Jets, Taus, and E_{miss}", *CMS Physics Analysis Summary* **PFT-09-001** (2009).

[14] CMS Collaboration, "Commissioning of the Particle-Flow Reconstruction in Minimum-Bias and Jet Events from pp Collisions at 7 TeV", *CMS Physics Analysis Summary* **PFT-10-002** (2010).

[15] CMS Collaboration, "Tau Commissioning with 7-TeV data", *CMS Physics Analysis Summary* **PFT-10-004** (2010).

[16] CMS Collaboration, "Measurement of Inclusive W and Z Cross Sections in pp Collisions $\sqrt{s}$=7 TeV", *JHEP* **1101** (2011) 080.

[17] T. Sjöstrand *et al. JHEP* **2006** (2006) 026.

[18] Z. Was *et al. Nucl. Phys. B, Proc. Suppl.* **98** (2001) 96.

[19] CMS Collaboration, "Tau Identification in CMS", *CMS Physics Analysis Summary* **TAU-11-001** (2011).

[20] CMS Collaboration, "Measurement of the Inclusive $Z \to \tau\tau$ Cross Section in pp Collisions at $\sqrt{s}$=7 TeV", *to be published*.

[21] J. S. Conway, "Nuisance Parameters in Likelihoods for Multisource Spectra", *submitted to Proceedings of PhyStat 2011* (2011) arXiv:hep-ex/1103.0354.

[22] LHC Higgs Cross Section Working Group Collaboration *arXiv:hep-ex/1101.0593* (2011).

[23] M. S. Carena et al., "MSSM Higgs Boson Searches at the Tevatron and the LHC: Impact of Different Benchmark Scenarios", *Eur. Phys. J.* (C45) 797–814.

[24] M. Spira, "HIGLU: A Program for the Calculation of the Total Higgs Production Cross Section at Hadron Colliders via Gluon Fusion including QCD Corrections", arXiv:hep-ph/9510347.

[25] S. Heinemeyer, W. Hollik, and G. Weiglein, "FeynHiggs: a program for the calculation of the masses of the neutral CP-even Higgs bosons in the MSSM", *Comput. Phys. Commun.* **124** (2000) 76–89, arXiv:hep-ph/9812320. doi:10.1016/S0010-4655(99)00364-1.

[26] R. V. Harlander and W. B. Kilgore, "Higgs boson production in bottom quark fusion at next-to- next-to-leading order", *Phys. Rev.* **D68** (2003) 013001, arXiv:hep-ph/0304035. doi:10.1103/PhysRevD.68.013001.

[27] S. Dittmaier, M. Kramer, and M. Spira, "Higgs radiation off bottom quarks at the Tevatron and the LHC", *Phys. Rev.* **D70** (2004) 074010, arXiv:hep-ph/0309204. doi:10.1103/PhysRevD.70.074010.

[28] S. Heinemeyer, W. Hollik, and G. Weiglein, "The Masses of the neutral CP - even Higgs bosons in the MSSM: Accurate analysis at the two loop level", *Eur. Phys. J.* **C9** (1999) 343–366, arXiv:hep-ph/9812472. doi:10.1007/s100529900006.

[29] G. Degrassi et al., "Towards high-precision predictions for the MSSM Higgs sector", *Eur. Phys. J.* **C28** (2003) 133–143, arXiv:hep-ph/0212020. doi:10.1140/epjc/s2003-01152-2.

[30] M. Frank et al., "The Higgs boson masses and mixings of the complex MSSM in the Feynman-diagrammatic approach", *JHEP* **02** (2007) 047, arXiv:hep-ph/0611326. doi:10.1088/1126-6708/2007/02/047.

Appendix 1 - Hadronic Tau Decay Identification

The tau identification algorithm used for this analysis is known as the Hadrons Plus Strips Algorithm (HPS). The HPS algorithm starts from a particle flow (PF) jet and reconstructs the possible tau decays inside the jet. The basic characteristic of the algorithm is that it uses azimuthal strips of clustered electromagnetic particles to account for brehmsstrahlung effects. Then the strips and charged hadrons are combined into the following categories:

1. Single hadron: This decay mode reconstructs single π/K tau decays or decays of type $\tau^- \to h^-\pi^0$ when the π^0 has very low energy.
2. Hadron plus strip: This type is aiming to reconstruct one-prong taus that are produced in association with a π^0 where the photons from the π^0 decay are very near in the calorimeter surface. The strip takes care of the possibility that one or both of those photons have converted.
3. Hadron plus two strips: This type is aiming to reconstruct one-prong taus that are produced in association with a π^0 where the photons from the π^0 decay are well separated in the calorimeter surface.
4. Three charged hadrons: This type is aiming to reconstruct the three-prong decays of taus. Three hadrons are required with a compatible total charge ($|q| = 1$) coming from a common vertex estimated by the Kalman vertex fit algorithm.

A constraint is applied on the strip mass to match the π^0 mass and the invariant mass of the hadron plus strip is calculated. This invariant mass should be compatible with the mass of the $\rho(770)$ resonance. The last step of the HPS reconstruction is calculation of the isolation. The isolation is calculated in a solid cone of $\Delta R = 0.5$ around the reconstructed tau decay mode axis. Isolation can use the energy sum of the PF objects or a count of PF objects above a certain threshold. All the PF objects in the cone are initially included in the isolation calculation but then the PF objects that correspond to the reconstructed tau are subtracted. This procedure is expected to provide better separation of taus and hadronic jets than an annulus-type isolation since it can separate taus from narrow jets with high electromagnetic, or hadronic energy fractions. Three working points for isolation are defined:

1. Loose isolation: Requires no PF charged candidates with $p_{\mathrm{T}} > 1.0\,\mathrm{GeV}/c$ and no PF gamma candidates with $E_{\mathrm{T}} > 1.5\,\mathrm{GeV}$.
2. Medium isolation: Requires no PF charged candidates with $p_{\mathrm{T}} > 0.8\,\mathrm{GeV}/c$ and no PF gamma candidates with $E_{\mathrm{T}} > 0.8\,\mathrm{GeV}$.
3. Tight isolation: Requires no PF charged candidates with $p_{\mathrm{T}} > 0.5\,\mathrm{GeV}/c$ and no PF gamma candidates with $E_{\mathrm{T}} > 0.5\,\mathrm{GeV}$.

We find that the loose isolation requirement yields the best search sensitivity for the $e\tau_h$ and $\mu\tau_h$ channels; this is the operating point used in the search presented in this note.

Appendix 2 - Tau Pair Invariant Mass Reconstruction

We describe here a novel algorithm called Secondary Vertex Fit (SVfit) for tau pair invariant mass reconstruction that utilizes a likelihood maximization for each event. The likelihood is composed of separate terms which represent probability densities of:

- tau decay final state phase space,

- matching between the momenta of neutrinos produced in the tau decays and the reconstructed missing transverse momentum,
- a regularization "p_T-balance" term which accounts for the effects from visible decay product acceptance cuts on the tau pair invariant mass,
- the compatibility of tau decay parameters with the position of reconstructed tracks and the known tau lifetime $c\tau = 87\ \mu$m.

The likelihood is maximized as a function of a set of parameters which fully describe the tau decay. The decay of a tau with visible four-momentum P_{vis} measured in the laboratory frame can be parametrized by three variables. The invisible neutrino momentum is fully determined by these parameters. The "opening angle" θ is defined as the angle between the boost direction of the tau lepton and the momentum vector of the visible decay products in the rest frame of the tau. The azimuthal angle of the tau in the lab frame is denoted as $\bar{\phi}$ (we denote quantities defined in the laboratory frame by a bar). A local coordinate system is defined such that the $\bar{z}$-direction lies along the visible momentum and $\bar{\phi} = 0$ lies in the plane spanned by the momentum vector of the visible decay products and the proton beam direction. The third parameter, $m_{\nu\nu}$, denotes the invariant mass of the invisible momentum system.

Given θ, $\bar{\phi}$, and $m_{\nu\nu}$, the energy and direction of the tau lepton can be computed by means of the following equations: The energy of the visible decay products in the rest frame of the tau lepton is related to the invariant mass of the neutrino system by:

$$E^{vis} = \frac{m_\tau^2 + m_{vis}^2 - m_{\nu\nu}^2}{2m_\tau}$$

Note that for hadronic decays, $m_{\nu\nu}$ is a constant of value zero, as only a single neutrino is produced. Consequently, the magnitude of E^{vis} depends on the reconstructed mass of the visible decay products only and is a constant during the SVfit.

The opening angle $\bar{\theta}$ between the tau lepton direction and the visible momentum vector in the laboratory frame is determined by the rest frame quantities via the (Lorentz invariant) component of the visible momentum perpendicular to the tau lepton direction:

$$\sin\bar{\theta} = \frac{p^{vis}\sin\theta}{\bar{p}^{vis}}$$

Given the parameters $m_{\nu\nu}$ and θ, the energy of the tau is obtained by solving for the boost factor γ in the Lorentz transformation of the visible momentum component parallel to the tau direction between the tau rest frame and the laboratory frame :

$$\bar{p}^{vis}\cos\bar{\theta} = \gamma\beta E^{vis} + \gamma p^{vis}\cos\theta$$

We include in the overall likelihood a term representing the phase space for tau decay, including the effect of the mass of the neutrino system in the leptonic decay cases, but ignoring (presently) the full matrix element for the individual decay mode.

The vectorial sum of the invisible transverse energy reconstructed by the SVfit is constrained to the measured $E_{\mathrm{T}}^{\mathrm{miss}}$. The likelihood is composed of two Gaussian terms corresponding to the components parallel and perpendicular to the the $\tau\tau$ momentum vector. The $E_{\mathrm{T}}^{\mathrm{miss}}$ resolutions used in the likelihood are measured in $Z \to \mu^+\mu^-$ events selected in the 7 TeV data collected by CMS in 2010.

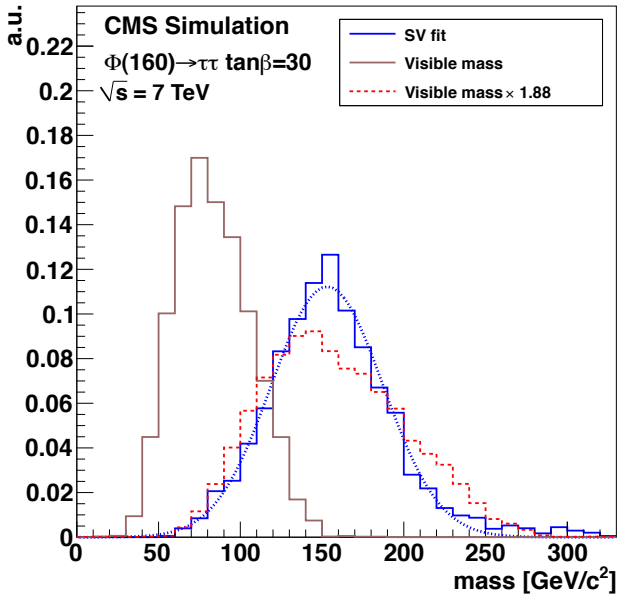

Figure 4: Tau pair mass reconstructed in simulated Higgs events with $m_A = 160$ GeV $/c^2$ by the SVfit (blue) compared to the to the visible mass (dark red). The red curve shows the visible mass scaled such that its mean value is the same as the SVfit mean value. The dotted line is a Gaussian function fitted to the SVfit spectrum.

In particular for tau lepton pairs produced in decays of resonances of low mass, the visible P_T cuts significantly affect the distribution of the momentum fraction $x = \frac{E_{vis}}{E_\tau}$ carried by visible decay products. To compensate for the effect of p_T threshold cuts on the spectra of reconstructed tau decay products, the SVfit algorithm likelihood also includes a term representing the probability density $p(p_T^\tau | m_{\tau\tau})$. This term in the likelihood is obtained from a parameterization of the simulated p_T^τ distribution in $Z/\Phi \to \tau\tau$ events as a function of $m_{\tau\tau}$. The inclusion of this term results in a significant improvement in resolution and in particular a significant reduction of the non–Gaussian tail in the region of high mass.

In additional to reconstructing the full mass of the tau pair, the SVfit algorithm has better relative resolution than the visible mass. The effect is illustrated in Fig. 4. The mass resolution is ∼21% at a Higgs mass of 130 GeV$/c^2$, to be compared with ∼24% for the (non-Gaussian) distribution of the invariant mass of the visible tau decay products.